

Integration of BT(R)DF Data into Radiance Lighting Simulation Programme

Technical Report
CTI Project 4881.1 “Bidirectional Goniophotometer”

Jerôme H. Kaempf
Physics/Computer Science Degrees UNIL

Jean-Louis Scartezzini, project leader
PhD, Physics Degrees UNIL/EPFL



CONTENTS

1	INTRODUCTION	5
2	METHODOLOGY	5
2.1	<i>BTDF(R)F Monitored Data.....</i>	<i>5</i>
2.2	<i>Radiance Software Routines</i>	<i>7</i>
3	DESCRIPTION OF <i>BTDF2PRISM2</i> PROCEDURE	9
3.1	<i>Transformation of BTDF data into transmission coefficients.....</i>	<i>9</i>
3.2	<i>Identification of prevailing emerging directions.....</i>	<i>10</i>
3.3	<i>Attribution of a transmission coefficient to the prevailing emerging directions.....</i>	<i>12</i>
3.4	<i>Attribution of spherical angular coordinates to the prevailing emerging directions</i>	<i>13</i>
3.5	<i>Use of symmetry properties of BTDF data.....</i>	<i>13</i>
4	IMPLEMENTATION OF <i>BTDF2PRISM2</i> PROCEDURE	15
4.1	<i>Utilisation of “prism2” generic material.....</i>	<i>15</i>
4.2	<i>Utilisation of a function file CAL.....</i>	<i>15</i>
4.3	<i>Utilisation of bidirectional properties of BTDF data</i>	<i>16</i>
4.4	<i>Improvement of rendering by sky vault sectors’ interpolation.....</i>	<i>16</i>
5	COMPUTER SIMULATION RESULTS	22
6	CONCLUSION	23
	REFERENCES	24

ANNEX A : BTDF/BRDF Data Format

ANNEX B : LCP CAL Interpretation File

1 INTRODUCTION

The characterisation of advanced fenestration systems by means of Bidirectional Transmission (or Reflection) Distribution Functions can significantly contribute to a more general use of daylighting technologies in buildings. The recent development of experimental devices that facilitate the monitoring of reliable and accurate BT(R)DF data (Andersen 2004) constitutes a major step toward the development of a standard assessment procedure of the photometrical features of these systems.

On the other hand, computer modelling of complex glazings and daylight redirecting devices (IEA 2000) offers an excellent platform for daylighting research and development (Ward 1997). The integration of monitored BT(R)DF data into daylighting simulation programmes enables more accurate rendering of daylight propagation through (or from) advanced fenestration systems.

This objective was addressed within the present project using the different advanced fenestration systems which were characterised by means of the novel EPFL bidirectional goniophotometer and the modelling capabilities offered by the Radiance Lighting simulation programme. The application developed for this purpose, together with simulation results of a particular fenestration system (laser cut panel), are given in this technical report. Moreover, advantages and limits of this approach are discussed.

2 METHODOLOGY

2.1 BTD(R)F Monitored Data

The Bidirectional Transmission (or Reflection) Distribution Function, abbreviated BT(R)DF, was defined by the Commission Internationale de l'Eclairage (CIE, 1977) as the "Quotient of luminance of the medium by the illuminance on the medium", measured in [$\text{Cd}\cdot\text{m}^{-2}\cdot\text{lux}^{-1}$].

It can be expressed analytically by Equation (2.1), assuming that a reference plane is defined by the considered advanced fenestration system:

$$BTDF(P, \vec{\omega}_i, \vec{\omega}_t) \doteq \frac{\left(\frac{d\phi_t(P, \vec{\omega}_t)}{d\vec{A} \cdot d\vec{\omega}_t} \right)}{\left(\frac{d\phi_i(P, \vec{\omega}_i)}{d\vec{A}} \right)} \equiv \frac{L(P, \vec{\omega}_t)}{E(P, \vec{\omega}_i)} \quad (2.1)$$

where the corresponding literal symbols, typical of the Radiance programme community (Ward 1997), are given as follows:

- P is a particular point chosen in the reference plane
- \vec{A} a vector normal to the reference plane

and

ω_i, ω_t [sr]	a solid angle labelled by subscript i for the incident light flux and t for the transmitted light flux (the reflection case is not considered for the sake of simplicity)
$L(P, \vec{\omega}_i)$ [$\text{cd}\cdot\text{m}^{-2}$]	the luminance observed at point P in the direction $\vec{\omega}_i$ for the transmitted light flux
$E(P, \vec{\omega}_i)$ [Lux]	the illuminance in the reference plane due to the impinging light flux
φ_i, φ_t [Lm]	are respectively the impinging and the transmitted light flux

BTDF experimental data, monitored by means of the novel EPFL bidirectional goniophotometer, were used with the aim of their integration in the Radiance lighting simulation programme: reference (Andersen 2004) gives a comprehensive description of this photometric device based on the CCD imaging technique.

Integration of the reflective photometrical properties of advanced materials was not considered in a first step in this project, despite the ability of the EPFL equipment to monitor BRDF data as well. The huge effort dedicated to this specific point by the computer image rendering community (e.g. rendering of textures for instance) has already made available a large set of modelling techniques that reproduce the reflective properties of materials. As a consequence, the Radiance software already benefits from it (Ward 1992).

The BTDF monitored data are characterised by a couple of degrees angular resolution for the (φ, θ) spherical coordinates: this remains constant for all directions of the emerging light flux within the hemisphere thanks to the use of CCD imaging techniques (no adaptation of angular resolution for fine “peaking” of transmission features).

The data are provided as ASCII files, according to a digital format described in Annex A. The number of BTDF data necessary to cover the overall hemisphere of emerging light flux depends on the angular dimension of the averaging sector given by:

$$\Omega_\varphi : (\varphi \pm \Delta res_\varphi) \text{ and } \Omega_\theta : (\theta \pm \Delta res_\theta) \quad (2.2)$$

The BTDF monitoring procedure regarding the incident light flux directions follows the discretisation of the sky vault suggested by Tregenza within the framework of the International Daylighting Monitoring Programme (Tregenza 1987): 145 incident directions are considered as a consequence. Their angular resolution is variable, in accordance with the corresponding sky luminance monitoring protocol.

Figure 2.1 shows the corresponding stereographic projection. A partition of “rectangular” sectors, defined according to Reinhardt (Reinhardt 2001), was used in this case to achieve a full pavement of the hemisphere (circular sectors sustained by a constant 11° angular sector in the original Tregenza format cover only 68% of the hemisphere).

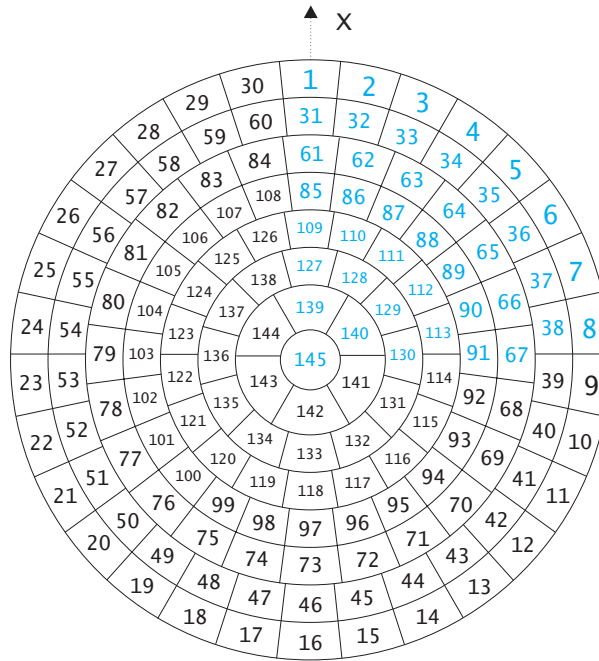


Figure 2.1: Stereographic projection of 145 Tregenza angular sectors (full partition by means of extended “rectangular” sectors)

2.2 Radiance Software Routines

The Radiance programme uses different generic functions to model the propagation of light in a building, taking into account its interaction with some specific materials (glazing panels, reflective surfaces, etc.): the user manual of the programme gives a comprehensive description of the generic functions (Ward 1997).

The “*prism2*” generic function was used and adapted to model the redirection of an impinging light beam by a complex fenestration system (prismatic film, holographic optical element, etc.) as implemented by Greenup et al. for laser cut panels (Greenup 2000). This function, which belongs to the “*materials*” subclass of the programme, was primarily designed to model the light redirecting impact of prismatic panels (Compagnon 1993). Two emerging directions, associated to the corresponding transmission coefficient, can be determined for each incident beam direction, as observed experimentally for prismatic panels: higher refraction orders, which lead to significantly lower light fluxes, are neglected as a consequence. The associated BTDF are approximated by two Dirac functions (δ -functions), weighted by transmission coefficients and oriented in the two prevailing directions of the refracted light beam.

According to the “*prism2*” specific function of the programme, the following two-step procedure is applied during the image rendering process:

- a) virtual sources associated to the two prevalent emerging directions are determined for each real source, which contributes significantly to the scene lighting (e.g. sunlight).
- b) light rays traced from the scene toward the virtual sources, which touch the glazing material, are re-directed toward the real source: a luminance value is then attributed to these rays taking account of the corresponding transmission coefficient in this direction (directional-directional) and the intensity of the source.

A global transmission coefficient (directional-hemispheric) is attributed to the rays traced through the “*prism2*” material that do not reach the virtual sources (e.g. light rays contributing to the direct vision of the outdoor environment through the fenestration system) in order to achieve an appropriate rendering.

Figure 2.2 gives a view of a computer simulation of a laser cut panel, carried out using the “*prism2*” material function. The modelling of the fenestration system does not rely on the use of monitored BRDF data in the Radiance programme: Descartes’ classical laws of optics and Fresnel equations are used to determine the two principal emerging directions of the impinging light flux together with the associated transmission coefficients (Greenup 2000).



Figure 2.2: Computer rendering of an office room equipped with a laser cut panel; modelling of fenestration system according to (Greenup 2000)

For the sake of simplicity, the “*prism2*” material function was also used in this project to model complex fenestration systems. The main programming effort concerned the elaboration of a procedure able to reduce BTDF monitored data of the fenestration material to the required “*prism2*” programming formalism: two principal emerging directions with associated transmission coefficients. This novel Radiance procedure, named *BTDF2prism2*, is described below.

3 DESCRIPTION OF *BTDF2PRISM2* PROCEDURE

The novel procedure, designed to translate monitored BTDF data into the appropriate “prism2” required format, was set up according to the following steps:

- a) Transformation of monitored BTDF data (expressed in [Cd·m.₂·lux.₋₁]) into transmission coefficients (directional–directional).
- b) Identification and separation of the two prevailing emerging directions of the light flux (interaction with the fenestration system) based on the monitored BTDF data (not applicable to highly diffusive materials).
- c) Attribution of a transmission coefficient to each prevailing emerging direction through a lumping up of the two “transmission peaks” (not applicable to highly diffusive materials).
- d) Attribution of a spherical angular coordinate to each prevailing emerging direction through the determination of the gravity centre of each “transmission peak”.

A comprehensive description of each step of procedure is given in this chapter.

3.1 Transformation of BTDF data into transmission coefficients

Due to the experimental monitoring procedure, each component of the BTDF data can be associated to a well defined hemispherical sector defined by Equation (2.2) and illustrated by Figure 2.1: Annex A gives a view of the distribution of these sectors of the whole hemisphere (2Π steradians).

As each component BTDF ($P, \vec{\omega}_i, \vec{\omega}_i$) is constant over these sectors, the transmission coefficients over the hemispherical sector defined by solid angle Ω_i :

$$\tau_{\Omega_i}(P, \vec{\omega}_i) = \int_{\Omega_i} BTDF(P, \vec{\omega}_i, \vec{\omega}) \cdot d\vec{\omega} \quad (3.1)$$

can be determined by means of a simple product given by Equation (3.2):

$$\tau_{\Omega_i}(P, \vec{\omega}_i) = BTDF(P, \vec{\omega}_i, \vec{\Omega}_i) \cdot \vec{\Omega}_i \quad (3.2)$$

By using the spherical coordinates defined from point P, Equation (3.2) can be expressed as follows:

$$\tau_{(\varphi_i, \theta_i)}(\varphi_i, \theta_i) = BTDF(\varphi_i, \theta_i, \varphi_i, \theta_i) \cdot \cos(\theta_i) \cdot \Omega_{(\varphi_i, \theta_i)} \quad (3.3)$$

where:

$$\Omega_{(\varphi_i, \theta_i)} = \left[\frac{2\pi \cdot (\cos(\theta_i + \Delta res_\theta / 2) - \cos(\theta_i - \Delta res_\theta / 2))}{\frac{2\pi}{\Delta res_\varphi}} \right]$$

Via a summation over the whole hemisphere Ω_h , one can get the directional-hemispherical transmission coefficient $\tau_h(\varphi_i, \theta_i)$, as shown in Equation (3.4):

$$\tau_h(\varphi_i, \theta_i) = \sum_{\Omega(\varphi_i, \theta_i) \in \Omega_h} BTDF(\varphi_i, \theta_i, \varphi_t, \theta_t) \cdot \cos(\theta_i) \cdot \Omega_{(\varphi_i, \theta_i)} \quad (3.4)$$

3.2 Identification of prevailing emerging directions

The procedure written in order to identify and separate the two prevailing emerging directions carefully examines a given set of BTDF data, using the following “pseudo-code”:

```

look for the maximal value in the data set, it belongs the peak 1
look for the neighbours of the maximal value, saved in neighbours of
peak 1
loop over the data set:
  look for the next maximal value in the data set
  if (it belongs to the neighbours of peak 1) add to peak 1 and re-
  evaluate the neighbours of peak 1
  else do:
    if (peak 2 exists and the maximal value belongs to the neighbours
    of peak 2) add to peak 2 and re-evaluate the neighbours of peak 2
    else if (peak 2 does not exist) create peak 2 and add the maximal
    value to peak 2, evaluate the neighbours of peak 2
    else add to the rest (not peak 1 and not peak 2)

until the end of the data set

```

In order to avoid taking into account unwanted noise, a minimal threshold value of 0.1% was applied to the transmission coefficients, filtering out the latter. In view of the accuracy of the novel goniophotometer, such a value is fully justified (Andersen 2004).

The next figures illustrate the identification and separation achieved by this procedure for three different complex glazings (IEA 2000):

- a laser cut panel
- a prismatic film
- a holographic optical element.

Figure 3.1 shows the typical symmetry along the axis defined by $\varphi = 180^\circ$ achieved by the laser cut panel. The first peak corresponds to the undeflected component of the transmitted light flux; the second to the deflected one, due to reflection (cf. Figure 2.2).

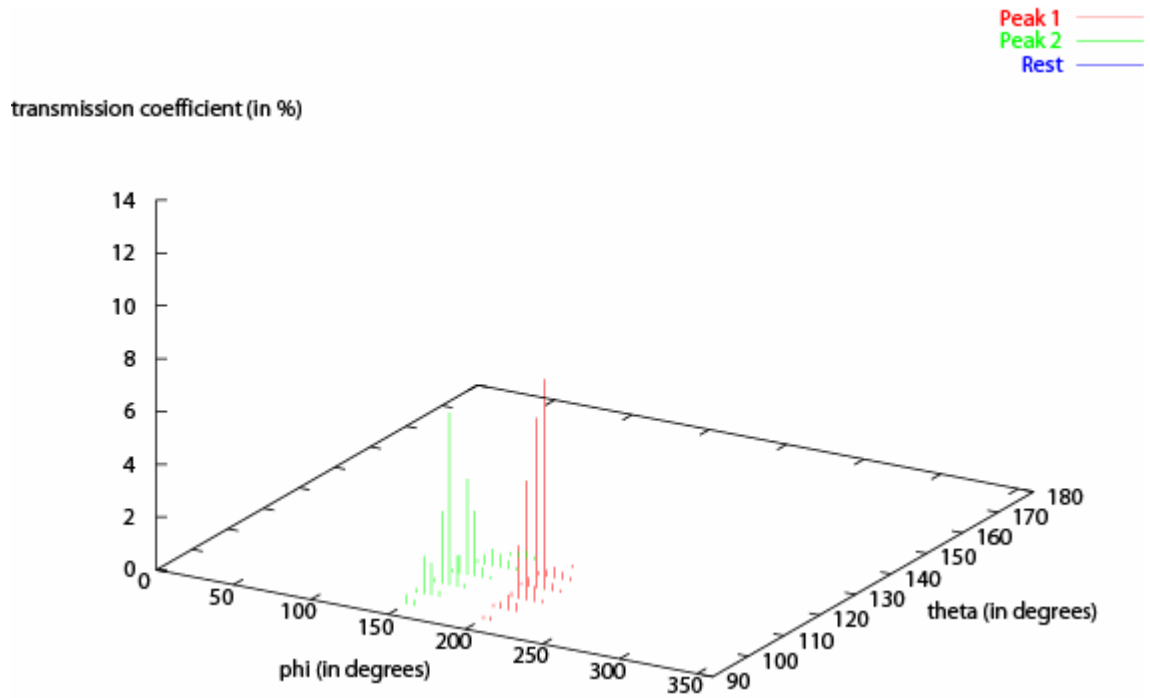


Figure 3.1: Transmission coefficient of laser cut panel for an impinging incidence of $(\varphi_i = 24^\circ, \theta_i = 72^\circ)$

Figure 3.2 illustrates the strong re-directing impact of a holographic optical element for an $(\varphi_i = 90^\circ, \theta_i = 12^\circ)$ impinging direction. The observed prevailing “peak transmission” values are larger than for any other glazing material, as diffraction tends to widen out the emerging light flux.

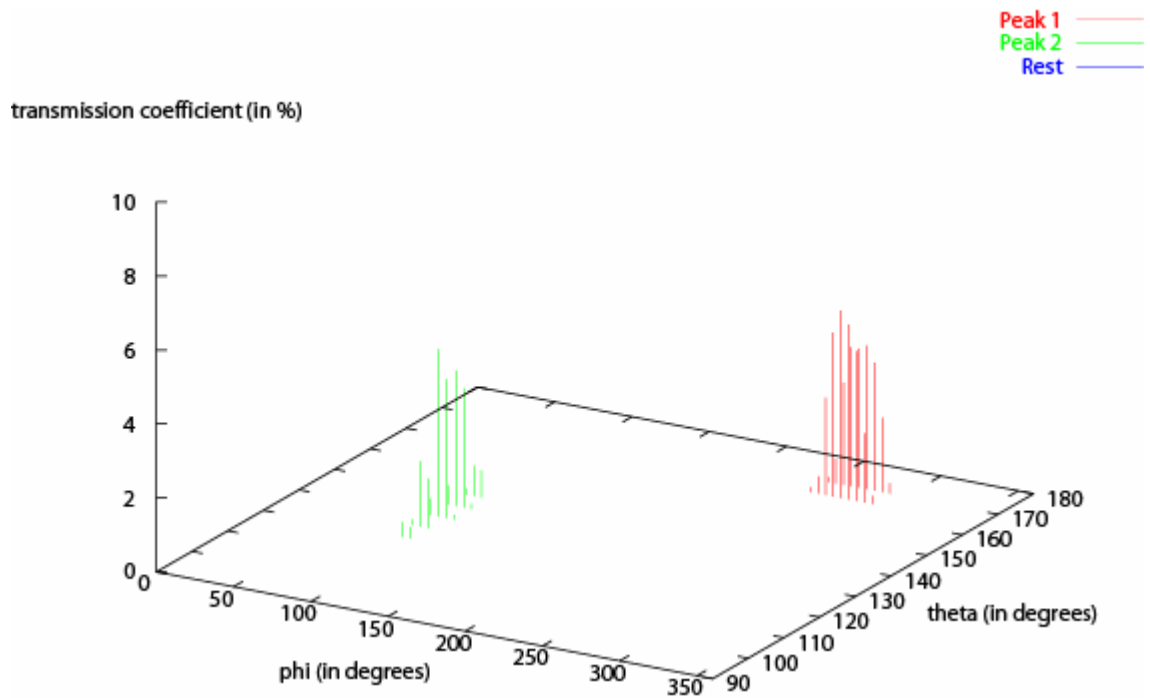


Figure 3.2: Transmission coefficient of holographic optical element for an impinging incidence of $(\varphi_i = 90^\circ, \theta_i = 12^\circ)$

Figure 3.3 shows the case of a prismatic film (3M OLF product). Two prevailing emerging directions appear in the figure, together with two smaller contributions (shown in blue). These two negligible contributions are not taken into account in the novel procedure based on the “*prism2*” function, as the number of emerging directions is limited to two.

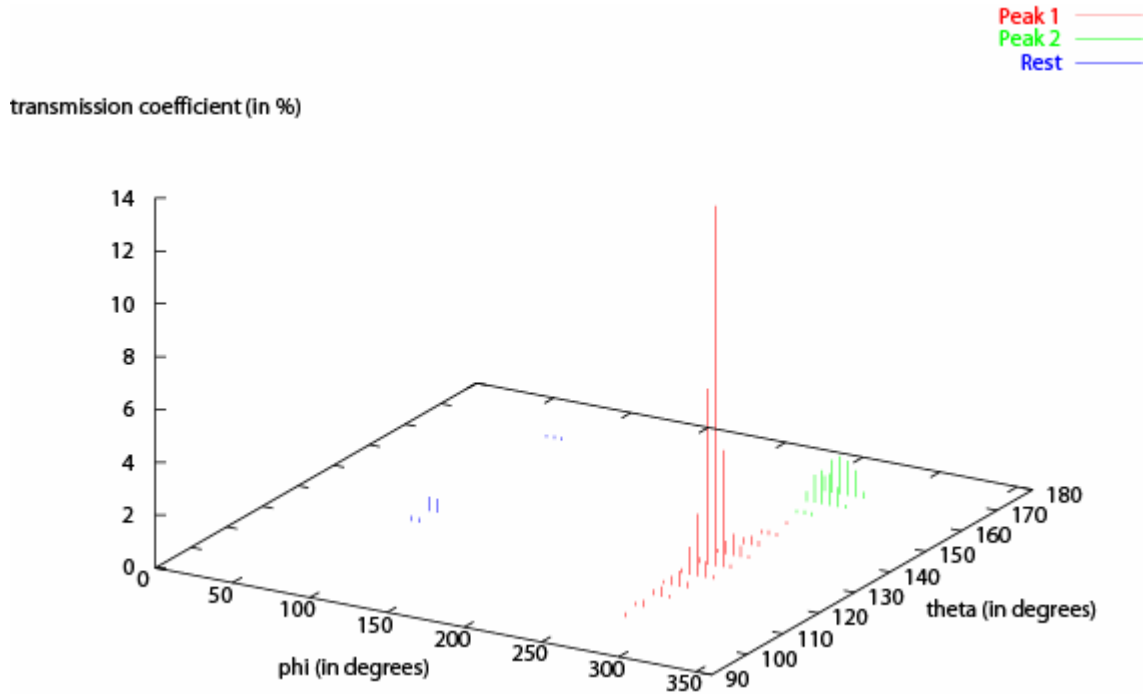


Figure 3.3: Transmission coefficients of prismatic film for an impinging incidence of $(\varphi_i = 90^\circ, \theta_i = 70^\circ)$

3.3 Attribution of a transmission coefficient to the prevailing emerging directions

To attribute a transmission coefficient to each prevailing emerging direction, the contribution of all the hemispherical sectors allocated to a given peak is summed up. By subtracting the coefficients obtained for each peak from the overall transmission coefficient of the considered panel (directional-hemispherical), a residual figure equal to the sum of the contributions of all sectors showing a transmission coefficient lower than the 0.1% threshold can be obtained.

The results obtained for the 3M prismatic film (35.2% and 11% “peak” transmission coefficient with a residue of 3.9%) are given below:

```

BTDF2prism2 v.2.0
Material: Film3M_Ext

Input Tregenza zone: 38 (phi_1: 90, theta_1:70)

Step in phi : 5 in theta : 5

Transmission: 51.8 %

Peak 1 : 35.2 %
Peak 2 : 11 %
Rest : 1.75 %

Under threshold: 3.9 %
(Threshold: 0.1 %)
    
```

3.4 Attribution of spherical angular coordinates to the prevailing emerging directions

The determination of the spherical angular coordinates of the two prevailing directions of the emerging light flux are calculated using the weighted mean method: Equation (3.5) was used for that purpose, leading to the corresponding $\bar{\theta}_{peak}(\varphi_i, \theta_i)$ and $\bar{\varphi}_{peak}(\varphi_i, \theta_i)$.

$$\bar{\varphi}_{peak}(\varphi_i, \theta_i) = \frac{\sum_{(\varphi, \theta) \in peak} BTDF(\varphi_i, \theta_i, \varphi, \theta) \cdot \varphi}{\sum_{(\varphi, \theta) \in peak} BTDF(\varphi_i, \theta_i, \varphi, \theta)} \quad (3.5)$$

$$\bar{\theta}_{peak}(\varphi_i, \theta_i) = \frac{\sum_{(\varphi, \theta) \in peak} BTDF(\varphi_i, \theta_i, \varphi, \theta) \cdot \theta}{\sum_{(\varphi, \theta) \in peak} BTDF(\varphi_i, \theta_i, \varphi, \theta)}$$

The case of the prismatic film, illustrated in Figure 3.2, is given below for a (90°, 70°) incident light beam. A (270°, 129°) direction was identified for the first one and (271°, 162°) was obtained for the second one.

```
BTDF2prism2 v.2.0

Material: Film3M_Ext

Input Tregenza zone: 38 (phi_1: 90, theta_1:70)

Step in phi : 5 in theta : 5

Transmission: 51.8 %

Peak 1 : 35.2 %
Position in (phi, theta): (270, 129)
Peak 2 : 11 %
Position in (phi, theta): (271, 162)

Rest : 1.75 %

Under threshold: 3.9 %
(Threshold: 0.1 %)
```

Beside the adaptation of the BTDF data to the configuration required by the “*prism2*” function, the symmetrical structure of some data was taken into account to further reduce the processing time.

3.5 Use of symmetry properties of BTDF data

Many complex glazing materials show properties of symmetry which are reflected by their BTDF data. These properties are usually taken into account during the monitoring: see (Andersen 2004) for more detail. Five different types of symmetry were identified, they are labelled from 0 to 4, as shown below.

Symmetry 0: No symmetry

Symmetry 1: Rotational symmetry

$$BTDF(t, \theta_i, \varphi, \theta) = BTDF(\varphi_i, \theta_i, \varphi, \theta) \quad \forall t \in [0, 2\pi[\quad (3.6)$$

Symmetry 2: Up/down symmetry

$$BTDF(2\pi - \varphi_i, \theta_i, (2\pi - \varphi) \bmod 2\pi, \theta) = BTDF(\varphi_i, \theta_i, \varphi, \theta) \quad \forall \varphi_i \in [0, \pi[\quad (3.7)$$

Symmetry 3: Left/right symmetry

$$BTDF((\pi - \varphi_i) \bmod 2\pi, \theta_i, (\pi - \varphi) \bmod 2\pi, \theta) = BTDF(\varphi_i, \theta_i, \varphi, \theta) \\ \forall \varphi_i \in \left[0, \frac{\pi}{2}\right] \cup \left[\frac{3}{2}\pi, 2\pi\right[\quad (3.8)$$

Symmetry 4: Up/down and left/right symmetry

$$BTDF(2\pi - \varphi_i, \theta_i, (2\pi - \varphi) \bmod 2\pi, \theta) = BTDF(\varphi_i, \theta_i, \varphi, \theta) \\ BTDF(\pi - \varphi_i, \theta_i, (\pi - \varphi) \bmod 2\pi, \theta) = BTDF(\varphi_i, \theta_i, \varphi, \theta) \\ BTDF(\varphi_i + \pi, \theta_i, (\varphi + \pi) \bmod 2\pi, \theta) = BTDF(\varphi_i, \theta_i, \varphi, \theta) \quad (3.9) \\ \forall \varphi_i \in \left[0, \frac{\pi}{2}\right[$$

By combining the symmetry order of the considered fenestration systems with the one of the sky vault discretisation defined by Tregenza (symmetry of order 6), an efficient calculation of the contribution of all the 145 sectors can be achieved. The following table illustrates the case of a 3M prismatic panel with a symmetry of order 4 (up/down and left/right symmetry).

```
Prism2 v.2.0

Material: Film3M_Ext
Symmetry: 4

Input Tregenza zone: 38 (phi_1: 90, theta_1:70)

Step in phi : 5 in theta : 5

Transmission: 51.8 %

Peak 1 : 35.2 %
Position in (phi, theta): (270, 129)

Peak 2 : 11 %
Position in (phi, theta): (271, 162)

Rest : 1.75 %

Under threshold: 3.9 %
(Threshold: 0.1 %)

Input Tregenza zone(s) : 38 39 53 54
```

4 IMPLEMENTATION OF *BTDF2PRISM2* PROCEDURE

4.1 Utilisation of “*prism2*” generic material

The material “*prism2*” is defined as follows in the Radiance user manual:

```
void prism2 id
9+ coef1 dx1 dy1 dz1 coef2 dx2 dy2 dz2 funcfile transform
0
n A1 A2 .. An
```

The variables defined for this material definition are:

<code>coef₁, coef₂</code>	transmission coefficients attributed to the prevailing emerging Directions 1 and 2
<code>dx₁, dy₁, dz₁</code>	Cartesian coordinates of the direction vector associated to Direction 1
<code>dx₂, dy₂, dz₂</code>	Cartesian coordinates of the direction vector associated to Direction 2
<code>funcfile</code>	function file (CAL file) interpreted in Radiance by a compiler, which calculates the transmission coefficients (<code>coef₁</code> , <code>coef₂</code>) and associated vectors (<code>dx₁</code> , <code>dy₁</code> , <code>dz₁</code>) and (<code>dx₂</code> , <code>dy₂</code> , <code>dz₂</code>) for a given light impinging direction
<code>A₁, A₂, ... A_n</code>	number of strings placed in memory by the CAL file interpreter (used in the <code>funcfile</code> calculation)
<code>transform</code>	rotation and/or translation applied in between the Radiance and the <code>funcfile</code> reference frame

The reference frame for the Cartesian coordinates is arbitrarily chosen, the z-axis pointing up, the y-axis pointing to the north and the x-axis defined according to the right-hand rule.

4.2 Utilisation of a function file CAL

The Cartesian coordinates and transmission coefficients associated to two prevailing emerging directions, calculated for the 145 incident directions defined by Tregenza’s discretisation, are stored in the `funcfile`: in other words, all the numerical figures extracted from the BTDF data (cf. Chapter 3) are accessible for the CAL file interpreter of the Radiance programme.

Arrays of real numbers of dimension (145 x 1) were used for that purpose, leading to the storage of 145 values for `coef1`, $\varphi_{peak\ 1}$ and $\theta_{peak\ 1}$ as well as for `coef2`, $\varphi_{peak\ 2}$ and $\theta_{peak\ 2}$: `coef1(88)` is the transmission coefficient of Transmission Peak 1 for a light beam impinging from the 88th Tregenza’s hemispherical sector. According to Radiance’s own procedural language, the corresponding array is defined as follows:

$$coef_1(x) = select(x, t_1, \dots, t_{145})$$

A subroutine integrated into the Radiance programme was written in order to be able to provide data corresponding to the incoming rays’ vectors during the `funcfile` calculation.

Input angles given in spherical coordinates are determined first using the function *zonefunc* (θ, φ), when given in degrees:

```
zonefunc(x,y)=if(x-90, 0,
if(x-78,1+floor((y*30/360)+0.5), if(x-66,31+floor((y*30/360)+0.5),
if(x-54, 61+floor((y*24/360)+0.5), if(x-42, 85+floor((y*24/360)+0.5),
if(x-30, 109+floor((y*18/360)+0.5), if(x-18, 127+floor((y*12/360)+0.5),
if(x-6, 139+floor((y*6/360)+0.5), 145 )))))));
```

The A_1, A_2, \dots, A_n string of numbers is used to set the $\varphi = 0$ axis relative to the panel. The spherical coordinates are then translated into Cartesian coordinates relative to the reference plane defined in Paragraph 4.1.

4.3 Utilisation of bidirectional properties of BTDF data

As the laws of optics allow a reverse of the light path, the bidirectional properties of BTDF data were used during the rendering process in order to take account of light rays travelling from inside to outside through the fenestration systems.

As a consequence, the *zonefunc* function was extended to define light rays input directions corresponding to the 145 Tregenza sectors on the inner side of the glazing panel. This extended function is given by:

```
zonefunc(x,y)=if(x-90, -if(180-x-78,1+floor((mod(180-y,360)*div(1)360)+0.5), if(180-x-
66,31+floor((mod(180-y,360) *div(2)/360)+0.5), if(180-x-54, 61+floor((mod(180-y,360)
*div(3)/360)+0.5, if(180-x-42, 85+floor((mod(180-y,360) *div(4)/360)+0.5), if(180-x-30,
109+floor((mod(180-y,360) *div(5)/360)+0.5), if(180-x-18, 127+floor((mod(180-y,360)*div(6)/360)+0.5),
if(180-x-6, 139+floor((mod(180-y,360) *div(7)/360+0.5, 145 ))))))), if(x-78,1+floor((y*30/360)+0.5,
if(x-66,31+floor((y*30/360)+0.5), if(x-54, 61+floor((y*24/360)+0.5, if(x-42,
85+floor((y*24/360)+0.5), if(x-30, 109+floor((y*18/360)+0.5), if(x-18, 127+floor((y*12/360)+0.5),
if(x-6, 139+floor((y*6/360)+0.5, 145 )))))));
```

Travelling directions of the emerging light flux had to be reversed in order to trace these rays and weight them by the transmission coefficient given by the corresponding BTDF data.

4.4 Improvement of rendering by sky vault sectors' interpolation

The discretisation of the sky vault according to Tregenza (Tregenza 1987) leads to the definition of 145 fixed space directions, which correspond to the centre of each discrete spherical sector. The extension of the original format toward “rectangular” sectors in order to achieve a full partition of the hemisphere did not modify these directions, which aim at the centroid of each rectangular sector.

No direct relationship exists between the 145 directions and the continuous curves traced by the sun course over the sky vault for different seasons. As a consequence, the evaluation of the direct daylight component (sunlight) through a fenestration system is slightly distorted by the use of Tregenza's discretisation compared to reality. In order to further improve the scene rendering, an angular interpolation procedure suggested by Reinhart within the framework of his thesis (Reinhart, 2001) was implemented in the programme to overcome this weakness.

The procedure is based on an appropriate modification of the original BTDF data by means of weighting factors that depend on the angular distances in-between a given sun position and the centroids of neighbouring sectors (cf. Figure 4.1). For each sun position on its course, the centroids of the four neighbouring sectors are determined by means of the following routine written for the CAL interpreter of the Radiance programme:

```
div(x)=select(x,30,30,24,24,18,12,6,1) ;

thetah = 90-signe*(floor((abs(90-theta2)-6)/12)*12+6);
thetab = 90-signe*(floor((abs(90-theta2)-6)/12 + 1)*12+6);

bandeh=floor(if(thetah-90, (thetah-90)/12 + 1, (90-thetah)/12 + 1));
bandeb=floor(if(thetab-90, (thetab-90)/12 + 1, (90-thetab)/12 + 1));

deltah=div(abs(bandeh));
deltab=div(abs(bandeb));

phidh = floor(phi2*deltah/360)*(360/deltah);
phigh = (floor(phi2*deltah/360)+1)*(360/deltah);
phidb = floor(phi2*deltab/360)*(360/deltab);
phigb = (floor(phi2*deltab/360)+1)*(360/deltab);
```

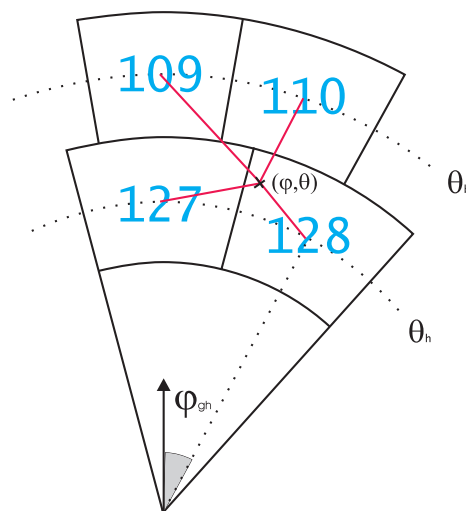


Figure 4.1: Neighbouring sectors and weighting factors of a given point on the sky vault located by (φ, θ) spherical coordinates

The function $div(x)$ determines the number of sectors of each of the eight spherical segments defined by Tregenza's discretisation of the sky vault (cf. Figure 2.1). The following parameters are used within this routing:

- | | |
|----------------|---|
| thetah, thetab | are respectively the upper and lower colatitude angles of the spherical segment which comprises the considered point of the sky vault |
| bandeh, bandeb | the cardinal of the spherical segments corresponding respectively to thetah and thetab |
| deltah, deltab | the number of sectors of the corresponding spherical segments |

phidh, phigh	the Euler angles of the centroids of the two neighbouring sectors located in the upper segment
phidb, phigb	the Euler angles of the centroids of the two neighbouring sectors located in the lower segment
theta2, phi2	the spherical coordinates of the considered sun position on the sky vault (equivalent to input data for the routine)

Four couples of (φ, θ) spherical coordinates, corresponding to the centroids of four neighbouring sectors, can be obtained by means of this routine: a call to the function *zonefunc* (x,y) can be used moreover to determine the cardinal number of these four spherical sectors within the 145 sectors of Tregenza's sky vault discretisation.

The spherical segments on the hemisphere measured between the considered sun position and the centroids of the four neighbouring sectors are used as weighting factors: Figure 4.1 illustrates this. Particular attention are paid to positions close to the zenith for which only three neighbouring sectors can be determined (cf. Figure 4.2).

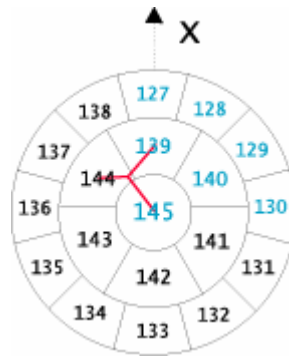


Figure 4.2: Sun position close to zenith with only three neighbouring sectors

The orthodromic distance is used to measure the length of the spherical segments between a pair of points located on the hemisphere. For two points P and N, this distance is determined through the scalar product of vectors \overrightarrow{OP} and \overrightarrow{ON} , whose origins are O the centre of the hemisphere. As the plane defined by the three points O, P and N cuts the hemisphere along a great circle, the orthodromic distance ψ measured in radians between vectors \overrightarrow{OP} and \overrightarrow{ON} can be determined using the equation:

$$\cos \psi = \frac{\overrightarrow{OP} \cdot \overrightarrow{ON}}{OP \cdot ON} \quad (4.1)$$

The two points P and N are expressed respectively in spherical coordinates (φ_P, θ_P) and (φ_N, θ_N) .

Taking account of the fact that the considered hemisphere is the unit sphere, Equation (4.1) can be rewritten as:

$$\cos \psi = \begin{pmatrix} \sin \theta_P \cdot \cos \varphi_P \\ \sin \theta_P \cdot \sin \varphi_P \\ \cos \theta_P \end{pmatrix} \cdot \begin{pmatrix} \sin \theta_N \cdot \cos \varphi_N \\ \sin \theta_N \cdot \sin \varphi_N \\ \cos \theta_N \end{pmatrix} \quad (4.2)$$

equivalent to:

$$\cos \psi = \sin \theta_P \cdot \sin \theta_N \cdot \cos(\varphi_P - \varphi_N) + \cos \theta_P \cdot \cos \theta_N \quad (4.3)$$

where ψ is measured in radians.

On the other side, the weighted transmission coefficients of the considered fenestration system is expressed as follows:

$$\frac{\text{coef}_{peak_i}}{\text{coef}_{peak_i}} = \frac{\sum_{K=1}^4 \omega_k \cdot (\text{coef}_{peak_i})_k}{\sum_{K=1}^4 \omega_k} \quad \forall i \in \{1,2\} \quad (4.4)$$

where

- ω are the weighting factors depending on orthodromic distance ψ
- $i \in \{1,2\}$ is the index corresponding to the two prevailing transmission “peaks” of the advanced glazing (cf. Figures 3.1 to 3.3)
- $k \in \{1,2,3,4\}$ is the index referring to the neighbouring sectors

The weighting of the colatitude angle θ is achieved using the following equation, which excludes angles corresponding to a transmission coefficient equal nil:

$$\frac{\theta_{peak_i}}{\theta_{peak_i}} = \frac{\sum_{K=1}^4 \omega_k \cdot \alpha_{ik} \cdot (\theta_{peak_i})_k}{\sum_{K=1}^4 \omega_k \cdot \alpha_{ik}} \quad \forall i \in \{1,2\} \quad (4.5)$$

where $\alpha_{ik} = \begin{cases} 1 & \text{if } (\text{coef}_{peak_i})_k > 0 \\ 0 & \text{otherwise} \end{cases} \quad \forall i \in \{1,2\} \quad \forall k \in \{1..4\}$

The corresponding expression for the Euler angle φ is given below. Four different regions, illustrated in Figure 4.3, are used to avoid φ spreading angles larger than 180°; they are taken into account in the following expression:

$$\bar{\varphi}_{peak_i} \left\{ \begin{array}{l} \frac{\sum_{K=1}^4 \omega_k \cdot \alpha_{ik} \cdot (\theta_{peak_i})_k}{\sum_{K=1}^4 \omega_k \cdot \alpha_{ik}} \quad \begin{array}{l} \text{if } (\forall k \in \{1..4\}) : \\ (\varphi_{peak_i})_k \in [0, \pi[\\ \vee (\varphi_{peak_i})_k \in \left[\frac{3}{2}\pi, \frac{5}{2}\pi \right[\\ \vee (\varphi_{peak_i})_k \in [\pi, 2\pi[\end{array} \\ \frac{\left[\left[\sum_{k=1}^4 \omega_k \cdot \alpha_{ik} \cdot ((\varphi_{peak_i})_k + \pi) \bmod 2\pi \right] + \pi \right] \bmod 2\pi}{\sum_{k=1}^4 \omega_k \cdot \alpha_{ik}} \quad \begin{array}{l} \text{if } (\forall k \in \{1..4\}) : \\ (\varphi_{peak_i})_k \in \left[0, \frac{\pi}{2} \right[\cup \left[\frac{3}{2}\pi, 2\pi \right[\end{array} \\ (\varphi_{peak_i})_{k \in (\text{primary Tregenza sector})} \quad \text{elsewhere} \end{array} \end{array} \right. \quad (4.5)$$

$\forall i \in \{1,2\}$

where the first term of Equation (4.5) corresponds to Regions 1,2 and 4 illustrated in the figure and the second term corresponds to Region 3.

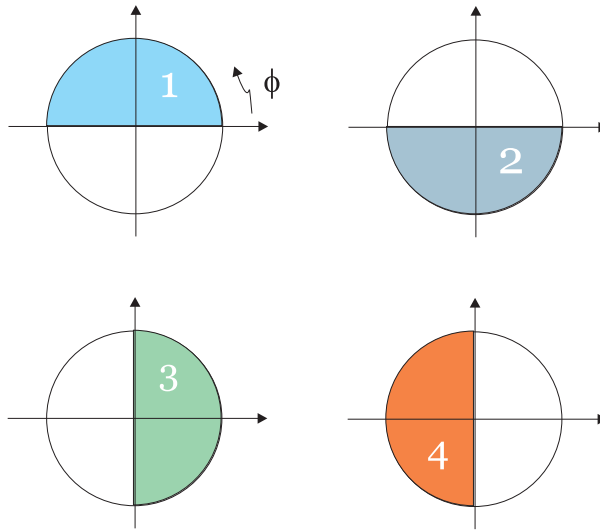


Figure 4.3: The four regions used in the $[0, 360^\circ[$ domain for weighting φ

Two simulation phases are distinguished in case the *prism2* material function of Radiance is used (see paragraph 2.2):

- a first pre-processing stage leading to the location of the virtual sources of the scene
- a second stage involving backward ray-tracing.

A digital flag was used in the programme in order to identify rays that hit the virtual sources. The CAL interpreter of the programme translates this information into a vector indicating the direction of the hit source (Dx_A , Dy_A , Dz_A); it is set to nil for directions of rays that do not hit a source. The following equation was used to define the corresponding flag:

$$flag = \sqrt{(Dx_A)^2 + (Dy_A)^2 + (Dz_A)^2} \quad (4.6)$$

A distinction is thus made in the backward ray tracing stage between rays hitting the considered glazing material, for which the output rays' direction is given, and rays hitting a virtual source, for which the source direction is provided.

5 COMPUTER SIMULATION RESULTS

An example of computer simulation of a laser cut panel (LCP) based on BTDF monitored data is given below.

A CAL interpreter file, showing all stages of the simulation procedure, is given as well (see Annex). The file ends with comments suggesting how it should be used with the *prism2* generic material of the Radiance programme.

A sequence of the scenes rendered for different sun positions is given in Figure 4.4 for the case of an LCP mounting in the upper part of a south oriented window. Spring equinox of March 21 was chosen for that purpose; the simulations were performed for a clear sky at a 47°N latitude using the Perez model (Perez 1993). The transmission features of this glazing panel can be observed in this figure: only a small fraction of impinging sunlight is regularly transmitted through the LCP panel, as the major part is redirected upward toward the ceiling. This is particularly visible in Figures 4.4 (c), (e) and (g), where it can be compared to the nearby regular transmission of the clear glass located in the lower window pane.

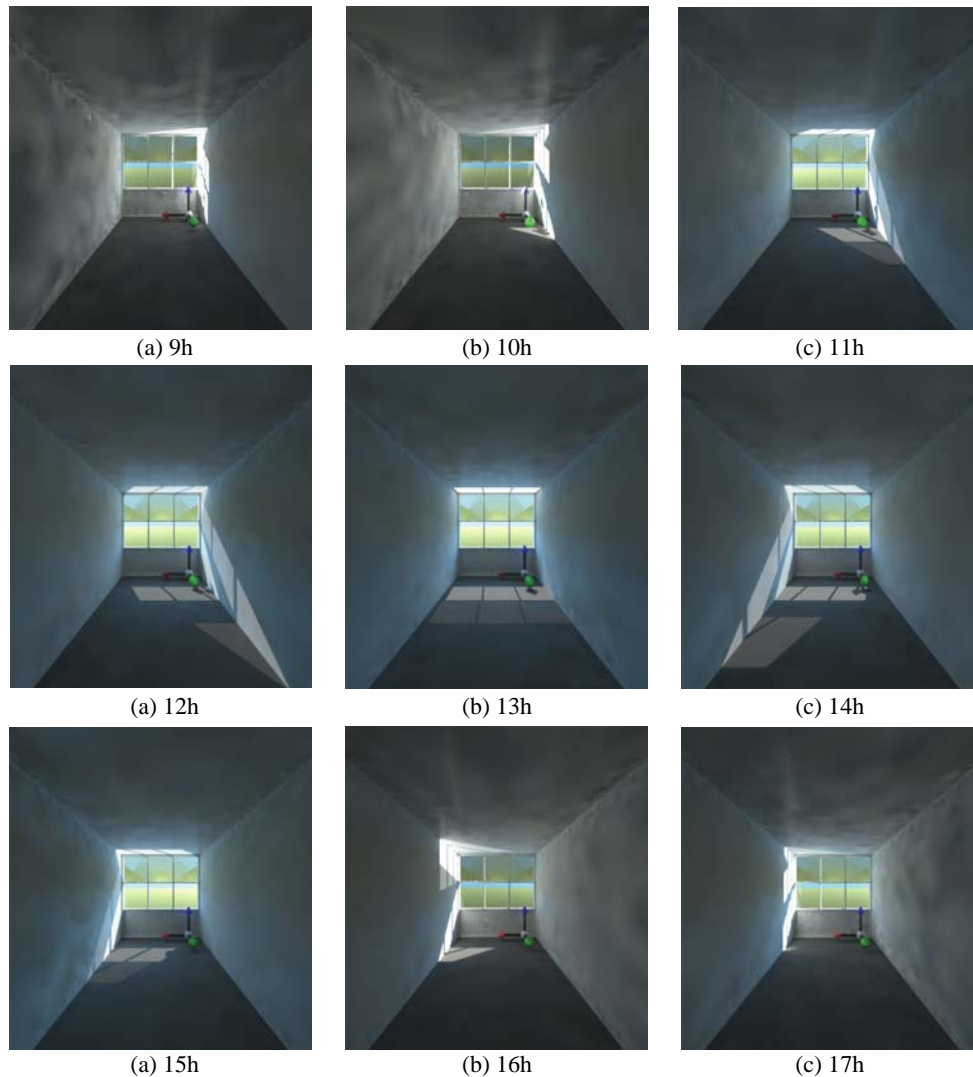


Figure 4.4: Radiance rendering of an LCP panel (upper window part) at different solar hours (47°N latitude, spring equinox, clear sky)

6 CONCLUSION

The integration of monitored BT(R)F data into daylight simulation programmes enables a more accurate rendering of light propagation through advanced fenestration systems. To meet this objective, experimental data generated by a novel bidirectional goniophotometer were used in conjunction with the modelling capabilities offered by the Radiance lighting simulation programme (Andersen 2004).

A new procedure, named *BTDF2prism2* was developed for that purpose. Based on the original *prism2* material generic function, it allows to simulate the light propagation through a complex fenestration system by accounting for the two prevailing emerging directions of the panel. Such directions are previously determined on the basis of the corresponding panel BTDF data after identification and separation of the prevailing emerging directions. Attribution of transmission coefficients and spherical coordinates to these two principal “transmission peaks” are made in order to fit the request of *prims2* input data. Further improvement of the rendering was achieved by means of interpolation for the different sun positions, which differ from the sky vault fixed directions imposed by Tregenza’s discretisation.

Renderings of a laser cut panel by means of this novel procedure confirmed the adequacy of the latter. It is believed that a majority of complex fenestration systems with rather particular transmission features can be modelled in an appropriate way using this novel Radiance procedure.

REFERENCES

- (Andersen 2004) M. Andersen, “Innovative Bidirectional Video-Goniophotometer for Advanced Fenestration Systems”, PhD Dissertation No 2941, EPFL, Lausanne (Switzerland), 2004-05-28.
- (CIE 1977) Commission Internationale de l’Eclairage, “Radiometric and Photometric Characteristics of Materials and their Measurement”, CIE 38(TC-2.3), 1977.
- (Compagnon 1993) R. Compagnon, “Numerical Simulations of Side Lighting Systems”, PhD Dissertation No 1193, Swiss Federal Institute of Technology (EPFL), Lausanne (Switzerland), 1993.
- (Greenup 2000) P.J. Greenup, I. Edmonds, R. Compagnon, “RADIANCE Algorithm to Simulate Laser-cut Panel Light Redirecting Elements”, Lighting Research and Technology, pp. 49-54, 32(2), 2000.
- (IEA 2000) International Energy Agency, “A Source Book on Daylighting Systems and Components”, IEA Solar Heating and Cooling Task 21, Published by LBNL, Berkeley (USA), 2000.
- (Perez 1993) R. Perez, R. Seals and J. Michalsky, “All-weather Model for Sky Luminance Distribution: Preliminary Configuration and Validation”, Solar Energy, 50(3), 235-245, 1993.
- (Reinhart 2001) C.F. Reinhart, “Daylight Availability and Manual Lighting Control in Office Buildings – Simulation Studies and Analysis of Measurements”, Thesis at the University of Karlsruhe, 2001.
- (Tregenza 1987) P.R. Tregenza, “Subdivision of the Sky Hemisphere for Luminance Measurements”, Lighting Research and Technology, pp. 13-14, 1987.
- (Ward 1992) G. Ward, “Measuring and Modelling Anisotropic Reflection”, ACM SIGGRAPH Computer Graphics, 26(2), pp. 265-272, 1992
- (Ward 1997) G. Ward, “The Radiance 3.1 Synthetic Imaging System”, Radiance Reference Manual, 1997

ANNEX A : BTDF/BRDF Data Format

DATA FORMAT for BTDF / BRDF measurements

Marilyne Andersen, LESO-PB / EPFL

Coordinate systems

The characterisation of a daylighting system with respect to different incident and emerging angles of the light flux requires the definition of a co-ordinate system, preferably based on international agreements.

Within the framework of Task 21 of the International Energy Agency, a common format was determined:

The **origin** of the co-ordinate system is placed on the daylighting component. Directions are defined by **spherical co-ordinates**: altitude angles θ_i and azimuth angles ϕ_i (see Fig. 1). Index i indicates whether it is related to the incident ($i = 1$) or transmitted / reflected ($i = 2$) direction.

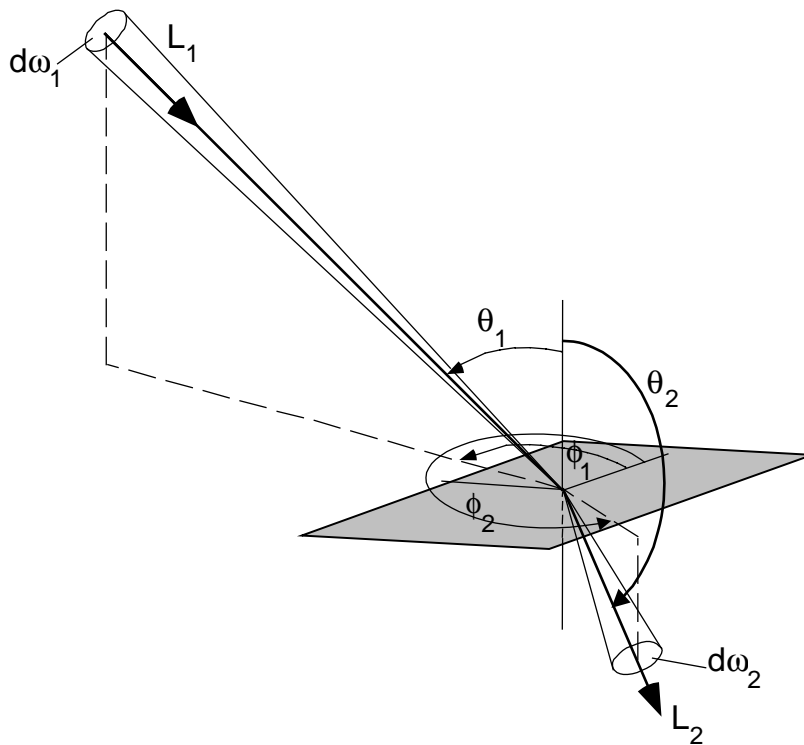


Fig. 1. Co-ordinate system for bi-directional measurements.

In order to avoid any confusion between files providing BTDFs and BRDFs (bi-directional reflection distribution functions), the altitude angle θ_2 is defined as the angle between the normal to the sample on the incident interface and the emerging light flux direction (see Fig. 1); it is therefore comprised between 0° and 90° for reflection, and between 90° and 180° for transmission. ϕ_1 and ϕ_2 are comprised between 0° and 360°

The relative position of a component to the co-ordinate system being of huge impact to the measurement results, the **orientation** of the sample must be precisely defined as well.

The following rules, illustrated by Fig. 2, apply to the adjustment:

- The sample plane is parallel to a vertical window plane (i.e. the z-axis, orthogonal to the sample element, points horizontally)
- If a particular direction appears on the sample, e.g. because of slats, colour lines, a prismatic shape, etc., the orientation of the sample within the x-y plane is defined in order to have this privileged direction collinear to direction $\phi_i = 0^\circ$ (see Fig. 2).
- The positive z-axis is the outside direction of the sample. The positive y-axis ($\phi_i = 90^\circ$) points out towards the top.

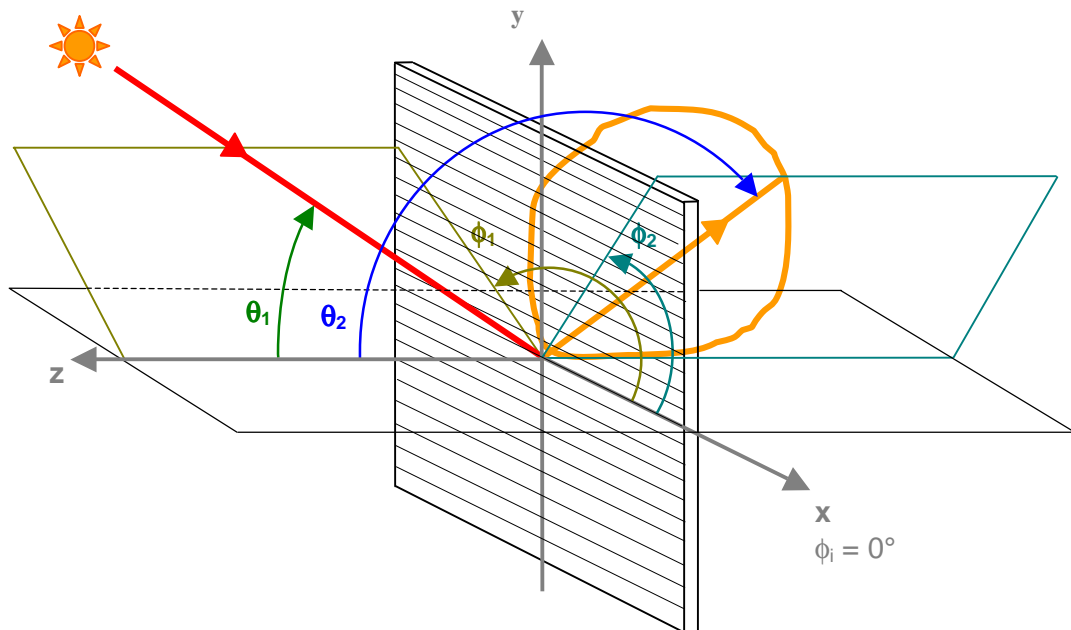


Fig. 2. Orientation of daylighting system with regard to the co-ordinate system.

Final electronic data:

The achieved BTDF/BRDF data set is saved in ASCII format on an electronic file denominated after the sample name, and including the institute's designation and the considered incident direction (e.g. les0_SampleName_theta_1_phi_1.txt).

This file contains the following data:

- the sample characteristics: name, manufacturer, symmetry indicator, area, thickness, eventual comments, date of measurement, institute denomination
- the measurement parameters: incident direction (θ_1, ϕ_1), output angular resolution ($\Delta\theta_2, \Delta\phi_2$), limit altitude θ_{lim} : this angle is the maximal altitude angle reachable without any obstruction due to mechanical components of the device.
- the hemispherical light transmittance $\tau(\theta_1, \phi_1)$, calculated through an integration of the BTDF values
- the BTDF/BRDF values, expressed in $[cd \cdot m^{-2} \cdot lx^{-1}]$, for each associated angular direction (θ_2, ϕ_2). The triplets $\phi_2, \theta_2, BTDF/BRDF$ are given in three columns separated by a tab character (ASCII code 9). As a result of image processing, the achieved data represent average values of the BTDFs/BRDFs measured in the output hemisphere regions limited by $(\phi_2 - \frac{1}{2}\Delta\phi_2; \phi_2 + \frac{1}{2}\Delta\phi_2)$ in azimuth and by $(\theta_2 - \frac{1}{2}\Delta\theta_2; \theta_2 + \frac{1}{2}\Delta\theta_2)$ in altitude for each outgoing direction. As a matter of fact, they do not only characterise the precise direction (θ_2, ϕ_2) to which they are associated, and can therefore vary according on the angular resolution ($\Delta\theta_2, \Delta\phi_2$).

An example of file contents is given below for BTDF values, which would be named "leso_Example_50_90.txt". The amount of data being of great importance for a sample, there is a single file for each light incidence.

```

#material: Example
#manufacturer: Unknown
#Isym = 0 ! symmetry indicator: 0 no symmetry (phi_1 = 0°...360°)
#      1 rotary symmetry (only for one phi_1)
#      2 symmetry to phi=0° and phi=180° (phi_1 = 0°...180°)
#      3 symmetry to phi=90° and phi=270° (phi_1 = -90°...90°)
#      4 symmetry to phi=0° and phi=180° & to phi=90° and phi=270° (phi_1 = 0°...90°)
#considered area [cm2]: 78.54
#thickness [cm]: 2.65
#comments: additional comments about the sample or the characterisation parameters
#measurements done at the Solar Energy and Building Physics Laboratory, LESO-PB/EPFL
#measurements and processing by Marilyne Andersen
#date of measurement: 08.03.00
#contact Marilyne.Andersen@epfl.ch for details
#light incidence :
#phi_1: 90° (azimuth)
#theta_1: 50° (altitude)
#BTDF values averaged over output directions from (phi_2 - 7.5) to (phi_2 + 7.5) in azimuth
#and from (theta_2 - 5.0) to (theta_2 + 5.0) in altitude
#measurements not performed for theta_2 < 95.0
#light transmittance: 0.09
#light transmittance calculated from BTDF values, with extrapolated values for 90 < theta_2 < 95.0
#data
#phi_2      theta_2  BTDF
0  100      0.030
15 100      0.028
30 100      0.018
45 100      0.021
60 100      0.021
75 100      0.018
... ..
315 100     0.018
330 100     0.016
345 100     0.028
0  110      0.030
15 110      0.030

[a.s.o.]
330 170     0.042
345 170     0.048
0  180      0.052
END

```

Default set of incident directions

It is agreed that the default set of incident directions conforms to the sky luminance distribution defined by Tregenza. This leads to 145 different light incidence directions which are shown on Fig. 3. If the sample presents any symmetry, the set of 145 directions can be reduced in a way described by Table 1.

Of course, depending on the manufacturer's desires, the incident directions set can be different from this configuration.

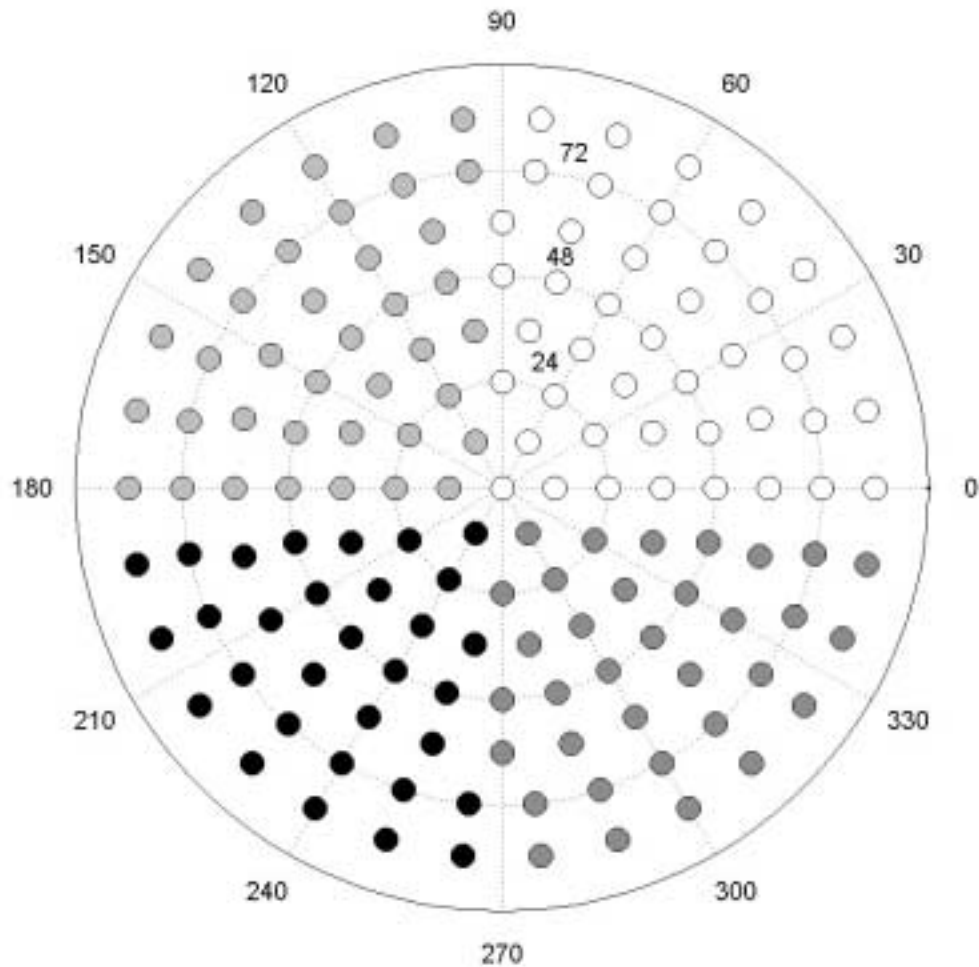


Fig. 3. Default set of 145 light incidence directions for bi-directional measurements, matching the subdivision of the sky hemisphere for luminance measurements defined by Tregenza. The grey levels associated to the different directions correspond to the backgrounds appearing in Table 1.

θ_1	ϕ_1 -step	ϕ_1	Light incidents must be measured for:
0°	-	0°	All samples
12°	60°	0°, 60°	All samples
24°	30°	0°, 30°, 60°, 90°	All samples
36°	20°	0°, 20°, 40°, 60°, 80°	All samples
48°	15°	0°, 15°, 30°, 45°, 60°, 75°, 90°	All samples
60°	15°	0°, 15°, 30°, 45°, 60°, 75°, 90°	All samples
72°	12°	0°, 12°, 24°, 36°, 48°, 60°, 72°, 84°	All samples
84°	12°	0°, 12°, 24°, 36°, 48°, 60°, 72°, 84°	All samples
<i>For rotational symmetry, only measurements for $\theta_1 = 0^\circ, 12^\circ, 24^\circ, 36^\circ, 48^\circ, 60^\circ, 72^\circ$ and 84° need to be done.</i>			
Additional Measurements, if the sample is asymmetric to:			
12°	60°	120°, 180°	$\phi_1 = 90^\circ / 270^\circ$
24°	30°	120°, 150°, 180°	$\phi_1 = 90^\circ / 270^\circ$
36°	20°	100°, 120°, 140°, 160°, 180°	$\phi_1 = 90^\circ / 270^\circ$
48°	15°	105°, 120°, 135°, 150°, 165°, 180°	$\phi_1 = 90^\circ / 270^\circ$
60°	15°	105°, 120°, 135°, 150°, 165°, 180°	$\phi_1 = 90^\circ / 270^\circ$
72°	12°	96°, 108°, 120°, 132°, 144°, 156°, 168°, 180°	$\phi_1 = 90^\circ / 270^\circ$
84°	12°	96°, 108°, 120°, 132°, 144°, 156°, 168°, 180°	$\phi_1 = 90^\circ / 270^\circ$
12°	60°	300°	$\phi_1 = 0^\circ / 180^\circ$
24°	30°	270°, 300°, 330°	$\phi_1 = 0^\circ / 180^\circ$
36°	20°	280°, 300°, 320°, 340°	$\phi_1 = 0^\circ / 180^\circ$
48°	15°	270°, 285°, 300°, 315°, 330°, 345°	$\phi_1 = 0^\circ / 180^\circ$
60°	15°	270°, 285°, 300°, 315°, 330°, 345°	$\phi_1 = 0^\circ / 180^\circ$
72°	12°	276°, 288°, 300°, 312°, 324°, 336°, 348°	$\phi_1 = 0^\circ / 180^\circ$
84°	12°	276°, 288°, 300°, 312°, 324°, 336°, 348°	$\phi_1 = 0^\circ / 180^\circ$
12°	60°	240°	$\phi_1 = 0^\circ / 180^\circ$ and $\phi_1 = 90^\circ / 270^\circ$
24°	30°	210°, 240°	$\phi_1 = 0^\circ / 180^\circ$ and $\phi_1 = 90^\circ / 270^\circ$
36°	20°	200°, 220°, 240°, 260°	$\phi_1 = 0^\circ / 180^\circ$ and $\phi_1 = 90^\circ / 270^\circ$
48°	15°	195°, 210°, 225°, 240°, 255°	$\phi_1 = 0^\circ / 180^\circ$ and $\phi_1 = 90^\circ / 270^\circ$
60°	15°	195°, 210°, 225°, 240°, 255°	$\phi_1 = 0^\circ / 180^\circ$ and $\phi_1 = 90^\circ / 270^\circ$
72°	12°	192°, 204°, 216°, 228°, 240°, 252°, 264°	$\phi_1 = 0^\circ / 180^\circ$ and $\phi_1 = 90^\circ / 270^\circ$
84°	12°	192°, 204°, 216°, 228°, 240°, 252°, 264°	$\phi_1 = 0^\circ / 180^\circ$ and $\phi_1 = 90^\circ / 270^\circ$

Table 1. Light Incidences based on the Tregenza configuration, accounting for sample symmetries.

ANNEX B : LCP CAL Interpretation File

```

{
    LaserCutPanel material

    prism2
    v. 2. 2
    22/05/02

    Jerome KAEMPF, LESO, EPFL
    jerome.kaempf@epfl.ch

    CAL file to compute virtual sources for re-direction with prism2

    input -
            A1 - x-coordinate of sample direction vector
            A2 - y-coordinate
            A3 - z-coordinate

    output -

    coef1      - transmission coefficient of major contribution
    dx1, dy1, dz1 - transmission direction for major contribution
    coef2      - transmission coefficient for minor contribution
    dx2, dy2, dz2 - transmission direction for minor contribution
    if forward pre-process stage to determine virtual sources

    DxA, DyA, DzA - direction to the real source
    if backward ray-tracing stage
}

c1(x)=select(x, 0. 185749, 0. 124978, 0. 0878785, 0. 0620332, 0. 0842579, . . . , 0. 803949);
p1(x)=select(x, 179. 368, 191. 187, 201. 451, 147. 045, 136. 669, 124. 114, . . . , 62. 6453);
t1(x)=select(x, 95. 249, 95. 5704, 98. 2458, 104. 852, 110. 017, 112. 758, . . . , 178. 016);
c2(x)=select(x, 0, 0. 0247649, 0. 0479909, 0. 00422616, 0. 00353045, . . . , 0. 0909997, 0);
p2(x)=select(x, 0, 169. 096, 158. 714, 161. 81, 145, 130, 249. 816, 262. 614, . . . , 180);
t2(x)=select(x, 0, 98. 1121, 101. 225, 120, 125, 130, 112. 065, 112. 934, . . . , 166. 552, 0);

{ Compute input angles on surface
    Nx, Ny, Nz      - surface normal
    Dx, Dy, Dz      - direction FROM target light source (badly
defined)
}

{ Calculation of NxA (N cross xprime) }
    NxAx = Ny*A3-Nz*A2;
    NxAy = Nz*A1-Nx*A3;
    NxAz = Nx*A2-Ny*A1;

{ Normalisation of N and D - normally not necessary }
    NormN = sqrt(Nx*Nx+Ny*Ny+Nz*Nz);
    NormD = sqrt(Dx*Dx+Dy*Dy+Dz*Dz);

{ Compute spherical angles associated to the reference frame attached to the panel }
    zz = (Nx*Dx+Ny*Dy+Nz*Dz);
    theta = acos(zz/(NormN*NormD));

{ The signe constant tells us on which side the ray is }
    signe = if(zz, 1., -1.);

{
    another way to calculate it

    costheta=abs(Rdot);
    theta = acos(costheta);
}

xx = (A1*Dx+A2*Dy+A3*Dz);
yy = (NxAx*Dx+NxAy*Dy+NxAz*Dz);
normxy = sqrt( xx*xx + yy*yy );

```



```

    phi = if( normxy, if( yy, (PI - acos( xx / normxy )), (PI + acos( xx /
normxy))), 0);
{ Conversion in degrees }
    theta2=theta*180/PI;
    phi 2=phi *180/PI;
{ Adjacent Tregenza zones }
    div(x)=select(x, 30, 30, 24, 24, 18, 12, 6, 1);
    thetah = 90-signe*(floor((abs(90-theta2)-6)/12)*12+6);
    thetab = 90-signe*(floor((abs(90-theta2)-6)/12 + 1)*12+6);
    bandeh=floor( if(thetah-90, (thetah-90)/12 + 1, (90-thetah)/12 + 1 ) );
    bandeb=floor( if(thetab-90, (thetab-90)/12 + 1, (90-thetab)/12 + 1 ) );
    del tah=div(abs(bandeh));
    del tab=div(abs(bandeb));
    phi dh = floor(phi 2*del tah/360)*(360/del tah);
    phi gh = (floor(phi 2*del tah/360)+1)*(360/del tah);
    phi db = floor(phi 2*del tab/360)*(360/del tab);
    phi gb = (floor(phi 2*del tab/360)+1)*(360/del tab);
{ Weight factors }
    fdh = acos( sin(thetah/180*PI)*sin(theta2/180*PI)*cos( (phi dh-phi 2)/180*PI ) +
cos(thetah/180*PI)*cos(theta2/180*PI ) );
    fgh = acos( sin(thetah/180*PI)*sin(theta2/180*PI)*cos( (phi gh-phi 2)/180*PI ) +
cos(thetah/180*PI)*cos(theta2/180*PI ) );
    fdb = acos( sin(thetab/180*PI)*sin(theta2/180*PI)*cos( (phi db-phi 2)/180*PI ) +
cos(thetab/180*PI)*cos(theta2/180*PI ) );
    fgb = acos( sin(thetab/180*PI)*sin(theta2/180*PI)*cos( (phi gb-phi 2)/180*PI ) +
cos(thetab/180*PI)*cos(theta2/180*PI ) );
{ A function to determine the Tregenza zone from theta and phi }
    zonefunc(x, y) =if(x-90, -if(180-x-78, 1+floor((mod(180-y, 360)*div(1)/360)+0.5),
if(180-x-66, 31+floor((mod(180-y, 360)*div(2)/360)+0.5), if(180-x-54, 61+floor((mod(180-
y, 360)*div(3)/360)+0.5), if(180-x-42, 85+floor((mod(180-y, 360)*div(4)/360)+0.5), if(180-
x-30, 109+floor((mod(180-y, 360)*div(5)/360)+0.5), if(180-x-18, 127+floor((mod(180-
y, 360)*div(6)/360)+0.5), if(180-x-6, 139+floor((mod(180-y, 360)*div(7)/360)+0.5), 145
)))))), if(x-78, 1+floor((y*30/360)+0.5), if(x-66, 31+floor((y*30/360)+0.5), if(x-54,
61+floor((y*24/360)+0.5), if(x-42, 85+floor((y*24/360)+0.5), if(x-30,
109+floor((y*18/360)+0.5), if(x-18, 127+floor((y*12/360)+0.5), if(x-6,
139+floor((y*6/360)+0.5), 145 ))))));
{ The 4 neighbouring zones and the usual zone }
    zone = zonefunc(theta2, phi 2);
    zone1 = zonefunc(thetab, phi gb);
    zone2 = zonefunc(thetah, phi gh);
    zone3 = zonefunc(thetah, phi dh);
    zone4 = zonefunc(thetab, phi db);
{ Coefficients associated to the combination of the 4 adjacent zones }
{ If zone=144 -> there is no difference in phi }
    pd1 = if(abs(zone1)-144, (1/(fgb+FTINY))/2 , (1/(fgb+FTINY)) );
    pd2 = if(abs(zone2)-144, (1/(fgh+FTINY))/2 , (1/(fgh+FTINY)) );
    pd3 = if(abs(zone3)-144, (1/(fdh+FTINY))/2 , (1/(fdh+FTINY)) );
    pd4 = if(abs(zone4)-144, (1/(fdb+FTINY))/2 , (1/(fdb+FTINY)) );
{ If the coefficient is zero, we don't use it for the weighted angles, but for the
weighted transmission coefficient }
    z1p1 = if(c1(abs(zone1)), 1., 0);
    z1p2 = if(c2(abs(zone1)), 1., 0);
    z2p1 = if(c1(abs(zone2)), 1., 0);
    z2p2 = if(c2(abs(zone2)), 1., 0);
    z3p1 = if(c1(abs(zone3)), 1., 0);
    z3p2 = if(c2(abs(zone3)), 1., 0);
    z4p1 = if(c1(abs(zone4)), 1., 0);
    z4p2 = if(c2(abs(zone4)), 1., 0);

```

```
{ The flag: forward pre-process or backward raytracing
```

```
  DxA, DyA, DzA are defined only in the backward raytracing bit, otherwise they are equal to 0 }
```

```
  flag = sqrt(DxA*DxA + DyA*DyA + DzA*DzA);
```

```
{ Interpolation }
```

```
{ Interpolation without bidirectionality
```

```
  coef1 = if(flag, (pd1*c1(abs(zone1)) +pd2*c1(abs(zone2)) +pd3*c1(abs(zone3)) +pd4*c1(abs(zone4)))/(pd1+pd2+pd3+pd4), if(sign, (pd1*c1(abs(zone1)) +pd2*c1(abs(zone2)) +pd3*c1(abs(zone3)) +pd4*c1(abs(zone4)))/(pd1+pd2+pd3+pd4), 0));  
  coef2 = if(flag, (pd1*c2(abs(zone1)) +pd2*c2(abs(zone2)) +pd3*c2(abs(zone3)) +pd4*c2(abs(zone4)))/(pd1+pd2+pd3+pd4), if(sign, (pd1*c2(abs(zone1)) +pd2*c2(abs(zone2)) +pd3*c2(abs(zone3)) +pd4*c2(abs(zone4)))/(pd1+pd2+pd3+pd4), 0));  
}
```

```
{ Output of the transmission coefficients }
```

```
  coef1 = (pd1*c1(abs(zone1)) +pd2*c1(abs(zone2)) +pd3*c1(abs(zone3)) +pd4*c1(abs(zone4)))/(pd1+pd2+pd3+pd4);  
  coef2 = (pd1*c2(abs(zone1)) +pd2*c2(abs(zone2)) +pd3*c2(abs(zone3)) +pd4*c2(abs(zone4)))/(pd1+pd2+pd3+pd4);
```

```
  post1 = (pd1*t1(abs(zone1))*z1p1 +pd2*t1(abs(zone2))*z2p1 +pd3*t1(abs(zone3))*z3p1 +pd4*t1(abs(zone4))*z4p1)/(pd1*z1p1+pd2*z2p1+pd3*z3p1+pd4*z4p1);  
  post2 = (pd1*t2(abs(zone1))*z1p2 +pd2*t2(abs(zone2))*z2p2 +pd3*t2(abs(zone3))*z3p2 +pd4*t2(abs(zone4))*z4p2)/(pd1*z1p2+pd2*z2p2+pd3*z3p2+pd4*z4p2);
```

```
{ Evaluation of interpolation region - p1 }
```

```
  sit1=if(p1(abs(zone1))-180 , if(p1(abs(zone2))-180 , if(p1(abs(zone3))-180 , if(p1(abs(zone4))-180, 2, 0), 0), 0) , if(180-p1(abs(zone2)) , if(180-p1(abs(zone3)) , if(180-p1(abs(zone4)), 1, 0), 0), 0));
```

```
  sit3 = if( 90-p1(abs(zone1)), if ( 90-p1(abs(zone2)) , if ( 90 - p1(abs(zone3)), if ( 90 -p1(abs(zone4)), 30, if ( p1(abs(zone4))-270, 30, 0)), if ( p1(abs(zone3)) - 270, if ( 90 -p1(abs(zone4)), 30, if ( p1(abs(zone4))-270, 30, 0)), 0) ), if ( p1(abs(zone2)) - 270, if ( 90 - p1(abs(zone3)), if ( 90 -p1(abs(zone4)), 30, if ( p1(abs(zone4))-270, 30, 0)), if ( p1(abs(zone3)) - 270, if ( 90 -p1(abs(zone4)), 30, if ( p1(abs(zone4))-270, 30, 0)), 0) ), 0) )  
  , if ( p1(abs(zone1))-270, if ( 90-p1(abs(zone2)) , if ( 90 - p1(abs(zone3)), if ( 90 - p1(abs(zone4)), 30, if ( p1(abs(zone4))-270, 30, 0)), if ( p1(abs(zone3)) - 270, if ( 90 -p1(abs(zone4)), 30, if ( p1(abs(zone4))-270, 30, 0)), 0) ), if ( p1(abs(zone2)) - 270, if ( 90 - p1(abs(zone3)), if ( 90 -p1(abs(zone4)), 30, if ( p1(abs(zone4))-270, 30, 0)), if ( p1(abs(zone3)) - 270, if ( 90 -p1(abs(zone4)), 30, if ( p1(abs(zone4))-270, 30, 0)), 0) ), 0) ), 0) );
```

```
  sit4 = if( p1(abs(zone1))-90 , if( 270-p1(abs(zone1)) , if( p1(abs(zone2))-90 , if(270-p1(abs(zone2)) , if(p1(abs(zone3))-90, if(270-p1(abs(zone3)) , if(p1(abs(zone4))-90, if(270-p1(abs(zone4)), 4, 0) , 0), 0), 0), 0) , 0) , 0) );
```

```
  sit = sit1+sit3+sit4;
```

```
{ Evaluation of interpolation region - p2 }
```

```
  sit1p2=if(p2(abs(zone1))-180 , if(p2(abs(zone2))-180 , if(p2(abs(zone3))-180 , if(p2(abs(zone4))-180, 2, 0), 0), 0) , if(180-p2(abs(zone2)) , if(180-p2(abs(zone3)) , if(180-p2(abs(zone4)), 1, 0), 0), 0));
```

```
  sit3p2= if( 90-p2(abs(zone1)) , if ( 90-p2(abs(zone2)) , if ( 90 - p2(abs(zone3)), if ( 90 -p2(abs(zone4)), 30, if ( p2(abs(zone4))-270, 30, 0)), if ( p2(abs(zone3)) - 270, if ( 90 -p2(abs(zone4)), 30, if ( p2(abs(zone4))-270, 30, 0)), 0) ) , if ( p2(abs(zone2)) - 270, if ( 90 - p2(abs(zone3)), if ( 90 -p2(abs(zone4)), 30, if ( p2(abs(zone4))-270, 30, 0)), if ( p2(abs(zone3)) - 270, if ( 90 -p2(abs(zone4)), 30, if ( p2(abs(zone4))-270, 30, 0)), 0) ), 0) )  
  , if ( p2(abs(zone1))-270, if ( 90-p2(abs(zone2)) , if ( 90 - p2(abs(zone3)), if ( 90 - p2(abs(zone4)), 30, if ( p2(abs(zone4))-270, 30, 0)), if ( p2(abs(zone3)) - 270, if ( 90 -p2(abs(zone4)), 30, if ( p2(abs(zone4))-270, 30, 0)), 0) ), if ( p2(abs(zone2)) - 270, if ( 90 - p2(abs(zone3)), if ( 90 -p2(abs(zone4)), 30, if ( p2(abs(zone4))-270, 30, 0)), if ( p2(abs(zone3)) - 270, if ( 90 -p2(abs(zone4)), 30, if ( p2(abs(zone4))-270, 30, 0)), 0) ), 0) ), 0) );
```

```

        sit4p2= if( p2(abs(zone1))-90 , if( 270-p2(abs(zone1)) , if( p2(abs(zone2))-90
        , if(270-p2(abs(zone2)) , if(p2(abs(zone3))-90, if(270-p2(abs(zone3))),
        if(p2(abs(zone4))-90, if(270-p2(abs(zone4))), 4, 0), 0), 0), 0), 0), 0 );

        sitp2 = sit1p2+sit3p2+sit4p2;

{ Evaluation of interpolation (phi) in the regions 1 to 4 }

posp1 = if ( sit - 30, (pd1*p1(abs(zone1))*z1p1 +pd2*p1(abs(zone2))*z2p1
+pd3*p1(abs(zone3))*z3p1
+pd4*p1(abs(zone4))*z4p1)/(pd1*z1p1+pd2*z2p1+pd3*z3p1+pd4*z4p1), if( 30 - sit, if( sit,
(pd1*p1(abs(zone1))*z1p1+pd2*p1(abs(zone2))*z2p1 +pd3*p1(abs(zone3))*z3p1
+pd4*p1(abs(zone4))*z4p1)/(pd1*z1p1+pd2*z2p1+pd3*z3p1+pd4*z4p1), p1(abs(zone)) ), mod(
(pd1*mod(p1(abs(zone1))+180, 360)*z1p1 +pd2*mod(p1(abs(zone2))+180, 360)*z2p1
+pd3*mod(p1(abs(zone3))+180, 360)*z3p1
+pd4*mod(p1(abs(zone4))+180, 360)*z4p1)/(pd1*z1p1+pd2*z2p1+pd3*z3p1+pd4*z4p1) + 180, 360)
));

posp2 = if ( sitp2 - 30, (pd1*p2(abs(zone1))*z1p2 +pd2*p2(abs(zone2))*z2p2
+pd3*p2(abs(zone3))*z3p2
+pd4*p2(abs(zone4))*z4p2)/(pd1*z1p2+pd2*z2p2+pd3*z3p2+pd4*z4p2), if( 30 - sitp2, if(
sitp2, (pd1*p2(abs(zone1))*z1p2+pd2*p2(abs(zone2))*z2p2 +pd3*p2(abs(zone3))*z3p2
+pd4*p2(abs(zone4))*z4p2)/(pd1*z1p2+pd2*z2p2+pd3*z3p2+pd4*z4p2), p2(abs(zone)) ), mod(
(pd1*mod(p2(abs(zone1))+180, 360)*z1p2 +pd2*mod(p2(abs(zone2))+180, 360)*z2p2
+pd3*mod(p2(abs(zone3))+180, 360)*z3p2
+pd4*mod(p2(abs(zone4))+180, 360)*z4p2)/(pd1*z1p2+pd2*z2p2+pd3*z3p2+pd4*z4p2) + 180, 360)
));

{
    posp1 = (pd1*p1(abs(zone1))*z1p1 +pd2*p1(abs(zone2))*z2p1 +pd3*p1(abs(zone3))*z3p1
+pd4*p1(abs(zone4))*z4p1)/(pd1*z1p1+pd2*z2p1+pd3*z3p1+pd4*z4p1); }
{
    posp2 = (pd1*p2(abs(zone1))*z1p2 +pd2*p2(abs(zone2))*z2p2 +pd3*p2(abs(zone3))*z3p2
+pd4*p2(abs(zone4))*z4p2)/(pd1*z1p2+pd2*z2p2+pd3*z3p2+pd4*z4p2); }

{ Transformation of the resulting angles }

    tt1 = (180-post1)*PI/180;
    pp1 = (360-posp1)*PI/180;

    tt2 = (180-post2)*PI/180;
    pp2 = (360-posp2)*PI/180;

{ Output of the re-directed components }

    dx1 = if( flag, DxA,
    signe*(A1*sin(tt1)*cos(pp1)+NxAx*sin(tt1)*sin(pp1)+Nx*cos(tt1));
    dy1 = if( flag, DyA,
    signe*(A2*sin(tt1)*cos(pp1)+NxAy*sin(tt1)*sin(pp1)+Ny*cos(tt1));
    dz1 = if( flag, DzA,
    signe*(A3*sin(tt1)*cos(pp1)+NxAz*sin(tt1)*sin(pp1)+Nz*cos(tt1));

    dx2 = if( flag, DxA,
    signe*(A1*sin(tt2)*cos(pp2)+NxAx*sin(tt2)*sin(pp2)+Nx*cos(tt2));
    dy2 = if( flag, DyA,
    signe*(A2*sin(tt2)*cos(pp2)+NxAy*sin(tt2)*sin(pp2)+Ny*cos(tt2));
    dz2 = if( flag, DzA,
    signe*(A3*sin(tt2)*cos(pp2)+NxAz*sin(tt2)*sin(pp2)+Nz*cos(tt2));

{ Sample of .rad file for simulation: }

{
void prism2 LaserCutPanel
9 coef1 dx1 dy1 dz1 coef2 dx2 dy2 dz2 LaserCutPanel.cal
0
3 1 0 0
}
{ Last parameters are the sample direction vector in Radiance coordinates }

```